NANO · MICRO small
www.small-journal.com

Valleytronics: Opportunities, Challenges, and Paths Forward

Steven A. Vitale, Daniel Nezich, Joseph O. Varghese, Philip Kim, Nuh Gedik, Pablo Jarillo-Herrero, Di Xiao, and Mordechai Rothschild*

A lack of inversion symmetry coupled with the presence of time-reversal symmetry endows 2D transition metal dichalcogenides with individually addressable valleys in momentum space at the *K* and *K′* points in the first Brillouin zone. This valley addressability opens up the possibility of using the momentum state of electrons, holes, or excitons as a completely new paradigm in information processing. The opportunities and challenges associated with manipulation of the valley degree of freedom for practical quantum and classical information processing applications were analyzed during the 2017 Workshop on Valleytronic Materials, Architectures, and Devices; this Review presents the major findings of the workshop.

1. Background

The Valleytronics Materials, Architectures, and Devices Workshop, sponsored by the MIT Lincoln Laboratory Technology Office and co-sponsored by NSF, was held in Cambridge, MA, USA on August 22–23, 2017. Valleytronics is an emerging field that promises transformational advances in information processing through the use of a particle's momentum index, possibly in conjunction with its charge and/or spin. Isolation of 2D materials such as graphene[1–3] and transition metal dichalcogenides (TMDs)[4,5] has allowed realization of experiments, which confirm our understanding of valley physics. However, development of useful devices for valleytronic computing or other technologies requires significant advancements in material quality, device designs, and circuit architectures.

Dr. S. A. Vitale, Dr. D. Nezich, Dr. J. O. Varghese, Dr. M. Rothschild
MIT Lincoln Laboratory
244 Wood Street, Lexington, MA 02421, USA
E-mail: steven.vitale@ll.mit.edu
Prof. P. Kim
Department of Physics
Harvard University
11 Oxford Street, Cambridge, MA 02138, USA
Prof. N. Gedik, Prof. P. Jarillo-Herrero
Department of Physics
Massachusetts Institute of Technology
77 Massachusetts Avenue, Cambridge, MA 02139, USA
Prof. D. Xiao
Department of Physics
Carnegie Mellon University
5000 Forbes Avenue, Pittsburgh, PA 15213, USA
The ORCID identification number(s) for the author(s) of this article can be found under https://doi.org/10.1002/smll.201801483.

DOI: 10.1002/smll.201801483

The workshop gathered the leading researchers in the field to present their latest work and to participate in honest and open discussion about the opportunities and challenges of developing applications of valleytronic technology. Three interactive working sessions were held, which tackled difficult topics ranging from potential applications in information processing and optoelectronic devices to identifying the most important unresolved physics questions. The primary product of the workshop is this article that aims to inform the reader on potential benefits of valleytronic devices, on the state-of-the-art in valleytronics research, and on the challenges to be overcome. We are hopeful this document will also serve to focus future government-sponsored research programs in fruitful directions. Though we provide some introduction to valley physics and to the state of existing knowledge, this article is not intended to be a comprehensive review of the literature. For that the reader is referred to several excellent review articles related to 2D materials and valleytronics.[6–13]

2. Introduction

When atoms brought together in close proximity form a crystal, the electrons of the constituent atoms interact with each other and with the atoms themselves, giving rise to distinct bands of energy that determine the electronic properties of the crystalline material. In semiconducting crystals, the bonding electrons populate a filled band of allowed states known as the valence band, and are separated from an unfilled band of higher energy known as the conduction band by an energy gap that contains no allowed states (the band gap). For some semiconductors, regions of minimum energy can appear in the conduction band that are indistinguishable from one another except for the direction of the crystal axes along which the energy band is oriented. Thus when carriers are excited across the band gap from the valence band into these minima in the conduction band, they will possess the same energy (be energy-degenerate), but will have differing crystal momenta depending on the orientations of the axes. These minima we refer to as valleys, and devices exploiting the fact that electrons, holes, or excitons (hereafter, particles) are present in one valley versus another we refer to as valleytronic devices. Selectively populating one momentum-distinguishable valley versus another—creating a valley polarization—is the key enabling feature of valleytronics.

The localization of a particle to a region of momentum space yields a new index by which to characterize it, namely, the valley pseudospin. This is in addition to the discrete spin index normally associated with a particle. Though energy-degenerate valleys are present in many periodic solids, it is usually impossible to address or manipulate particles in one valley independently from another as the valley state of a particle does not strongly couple to an applied external force. Thus it is impractical to construct useful valleytronic devices out of most materials. This is in contrast to spintronics, for example, where the electron spin is readily manipulated by magnetic fields through the electron spin magnetic moment or (less easily) by electric fields through spin–orbit coupling. For valleytronics to be useful, it is also of paramount importance that the particles populating a valley reside there for long enough to perform a desired function.

In some materials anisotropy of the particle mass along different crystal orientations can result in valley polarization under an applied field; preferential scattering occurs from one valley to another. This has been shown in diamond, aluminum arsenide, silicon, and bismuth at cryogenic temperatures. However, these materials still lack a strong coupling between the valley index and an external field. It is not possible to selectively initialize, manipulate, and readout particles in a specific valley. So we do not consider these materials in our discussion of valleytronics.

Fortunately, a class of materials does exist in which the valley pseudospin can be more readily addressed. In stark contrast to all other materials, 2D materials such as graphene and monolayer molybdenum disulfide possess valleys at the inequivalent K and K' points in the Brillouin zone (**Figure 1**), which exhibit strong valley-selective interactions with applied electric and magnetic fields. The isolation and investigation of these materials were seminal events in the field of valleytronics. As one can see in the histogram of publications in the field in **Figure 2**, the isolation of graphene in 2004 catalyzed new research in valley physics, but investigations into the optical properties of TMD monolayers in 2010 caused an explosion in the number of valleytronic publications.

The following discussion explains why some fundamental symmetries of monolayer materials are critical to valley addressability; it is largely based on published work.[13–15] We first elaborate on these symmetries and some valley-related concepts to clarify them for the reader.

In order to selectively couple to distinct valley states, it is necessary that there exist physical quantities that can distinguish between them. One such quantity is the Berry curvature, $\boldsymbol{\Omega}$. The Berry curvature describes the geometric properties of the electronic bands, and is central to the understanding of band topology-related effects. When describing the motion of electrons in crystal lattices, the semiclassical equations of motion are typically used, in which an electron is treated as a Bloch wave that can propagate through the crystal, and the mean velocity is proportional to the gradient of the electronic energy of the band. The periodicity of the lattice is taken into account (by the Bloch form of the electron wavefunction), as well as the response of the carriers to applied electric and magnetic fields. However, an additional contribution exists that is sometimes ignored—an anomalous velocity can appear that is proportional to the Berry curvature of an electronic band, and is established transverse to the applied electric field. This is of fundamental importance as it can allow valley currents and related phenomena to manifest in materials with nonvanishing Berry curvature.

Another physical quantity that can be used to distinguish valley states is the orbital magnetic moment, $\boldsymbol{m}$. Intuitively, it can be regarded as due to the self-rotation of an electron

Steven A. Vitale is a Senior Member of the Technical Staff at MIT Lincoln Laboratory. His research interests include novel devices for information processing, diamond transistors, ultra-low power computation, and plasma processing of advanced materials. Prior to Lincoln Laboratory, he developed front-end plasma processes at Texas Instruments for the 90–45 nm CMOS silicon technology nodes. He holds a Ph.D. in chemical engineering from MIT, an M.S. in nuclear engineering from MIT, and a B.S. in chemical engineering from Johns Hopkins University.

Daniel Nezich is a technical staff member at MIT Lincoln Laboratory. He received his B.S. in physics (2003) at Michigan Technological University and Ph.D. in physics (2010) at the Massachusetts Institute of Technology. He specializes in low-dimensional material growth, processing, and characterization in systems including carbon nanotubes, graphene, and transition metal dichalcogenides.

Joseph O. Varghese received his B.E. degree in chemical engineering from Cooper Union, and his Ph.D. degree in chemical engineering from the California Institute of Technology. His previous work includes the design and fabrication of thermoelectric nanostructures, and scanning probe and opto-electronic investigations of nanoscale materials. He is presently a member of the Technical Staff at MIT Lincoln Laboratory where his research interests include 2D valleytronic materials and the development of diamond transistor devices.

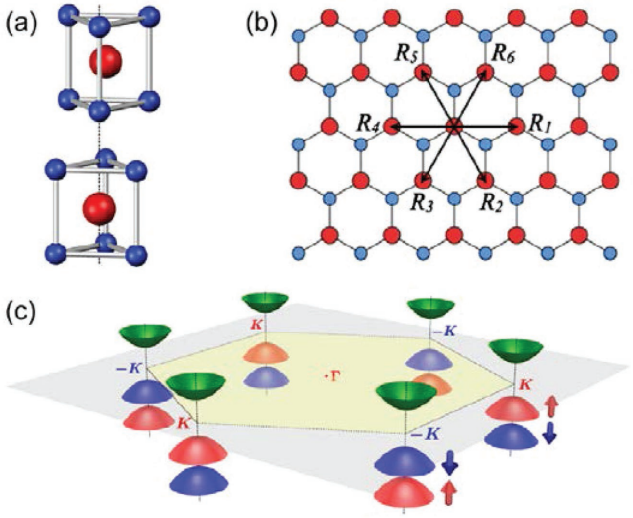

Figure 1. TMD crystal structure and Brillouin zone. a) the trigonal prismatic unit cell of non-inversion-symmetric TMDs, b) top-down view of the hexagonal lattice, c) first Brillouin zone with parabolic lowest conduction band and spin-orbit split valence band highlighted. Reproduced with permission.[14] Copyright 2012, the American Physical Society.

wavepacket. It is particularly useful since one can use it to discriminate between valley states in ways similar to experiments that exploit the spin magnetic moment of a charge carrier (for example, a magnetic field can differentiate between spin-up and spin-down states since they have opposite magnetic moments). The Berry curvature and orbital magnetic moment and one's ability to use them to distinguish valley states can however, vanish, if two types of symmetry simultaneously exist in a crystal—time-reversal symmetry and inversion symmetry.

In general, time-reversal symmetry refers to the symmetry of a system under a reversal of the sign of the time, while spatial inversion symmetry refers to symmetry under a reversal of the direction of all the coordinate axes. These simple symmetries have far-reaching consequences. Pseudovectors—such as the Berry curvature and the orbital magnetic moment—do not change sign under spatial inversion. Thus, one cannot

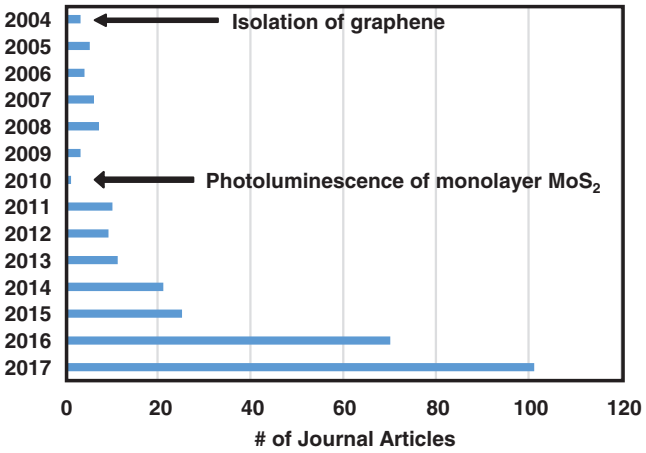

Figure 2. Number of relevant publications per year with "Valley" or "Valleytronic" in the title from the Compendex and Inspec databases.

use a pseudovector such as the Berry curvature to distinguish between valleys if inversion symmetry and time-reversal symmetry are simultaneously present, as it would vanish identically. The K and K' points in hexagonal 2D materials are time-reversed images of one another, so in general physical qualities that have odd parity under time reversal are good candidates to distinguish valley states. If at the K and K' points the Berry curvature and orbital magnetic moment are nonequivalent, one can in principle distinguish between the valleys using electric and magnetic fields, respectively. This is shown below.

The semiclassical equations of motion for Bloch electrons under applied electric and magnetic fields with nonvanishing Berry curvature are

$$\dot{\boldsymbol{r}} = \frac{1}{\hbar}\frac{\partial E_n(\boldsymbol{k})}{\partial \boldsymbol{k}} - \dot{\boldsymbol{k}} \times \boldsymbol{\Omega}_n(\boldsymbol{k}) \tag{1}$$

$$\hbar\dot{\boldsymbol{k}} = -e\boldsymbol{E} - e\dot{\boldsymbol{r}} \times \boldsymbol{B} \tag{2}$$

where $\boldsymbol{\Omega}$ can be defined in terms of the Bloch functions

$$\boldsymbol{\Omega}_n(\boldsymbol{k}) = \nabla_{\boldsymbol{k}} \times \boldsymbol{A}_n(\boldsymbol{k}) \tag{3}$$

$$\boldsymbol{A}_n(\boldsymbol{k}) = i\int u_n^*(\boldsymbol{r},\boldsymbol{k})\nabla_{\boldsymbol{k}} u_n(\boldsymbol{r},\boldsymbol{k})d^3\boldsymbol{r} \tag{4}$$

A_n is the Berry connection and u_n is the periodic part of the Bloch electron wavefunction in the nth energy band. The Berry curvature can also be written as

$$\boldsymbol{\Omega}_n(\boldsymbol{k}) = i\frac{\hbar^2}{m^2}\sum_{i\neq n}\frac{\boldsymbol{P}_{n,i}(\boldsymbol{k})\times\boldsymbol{P}_{i,n}(\boldsymbol{k})}{\left[E_n^0(\boldsymbol{k}) - E_i^0(\boldsymbol{k})\right]^2} \tag{5}$$

where $E_n^0(\boldsymbol{k})$ is the energy dispersion of the nth band, and $\boldsymbol{P}_{n,i}(\boldsymbol{k}) = \langle u_n|v|u_i\rangle$ is the matrix element of the velocity operator. By demanding that the equation of motion must remain invariant under the system symmetry, one can see that with time-reversal symmetry, $\boldsymbol{\Omega}_n(\boldsymbol{k}) = -\boldsymbol{\Omega}_n(-\boldsymbol{k})$, and with inversion symmetry $\boldsymbol{\Omega}_n(\boldsymbol{k}) = \boldsymbol{\Omega}_n(-\boldsymbol{k})$. Thus only when inversion symmetry is broken can valley-contrasting phenomena manifest. From the equations of motion we see that if an in-plane electric field is applied in a 2D crystal then a nonzero Berry curvature results in an anomalous electron velocity perpendicular to the field, and the velocity would have opposite sign for electrons in opposite valleys.

The broken inversion symmetry also allows the existence of the orbital magnetic moment. The electron energy dispersion in the nth band is modified to

$$E_n(\boldsymbol{k}) = E_n^0(\boldsymbol{k}) - \boldsymbol{m}_n(\boldsymbol{k})\cdot\boldsymbol{B} \tag{6}$$

where the quantity $\boldsymbol{m}$ is the orbital magnetic moment, given by

$$\boldsymbol{m}(\boldsymbol{k}) = i\frac{e\hbar}{2m^2}\sum_{i\neq n}\frac{\boldsymbol{P}_{n,i}(\boldsymbol{k})\times\boldsymbol{P}_{i,n}(\boldsymbol{k})}{E_n^0(\boldsymbol{k}) - E_i^0(\boldsymbol{k})} \tag{7}$$

Finite $\boldsymbol{m}$ is responsible for the anomalous g factor of electrons in semiconductors, which manifests itself in a shift of Zeeman energy in the presence of a magnetic field.

The existence of finite orbital magnetic moment also suggests that the valley carriers will possess optical circular dichroism, i.e., they will exhibit different properties upon illumination with right or left-circularly polarized light.[16–18] Though optical circular dichroism is also present in systems with broken time-reversal symmetry, it should be understood that the underlying physics in valleytronic materials is quite different and the dichroism is present even when time-reversal symmetry is maintained. One effect of the orbital magnetic moment is valley optical selection rules.[14]

As a specific example, the 2H phase of many 2D transition metal dichalcogenides lacks inversion symmetry and as a result exhibits contrasting $\boldsymbol{\Omega}$ and $\boldsymbol{m}$ between the K and K' valleys. The $\boldsymbol{k}\cdot\boldsymbol{p}$ Hamiltonian at the band edges in the vicinity of K and K' is given by

$$\hat{H} = at\left(\tau_z k_x \sigma_x + k_y \sigma_y\right) + \frac{\Delta}{2}\sigma_z \tag{8}$$

where a is the lattice spacing, t is the nearest-neighbor hopping integral, $\tau_z = \pm 1$ is the valley index, σ is the Pauli matrix element, and Δ is the band gap. In this case the Berry curvature in the conduction band is given by

$$\boldsymbol{\Omega}_c(k) = -\hat{z}\frac{2a^2t^2\Delta}{\left(4a^2t^2k^2 + \Delta^2\right)^{3/2}}\tau_z \tag{9}$$

Because of the finite Berry curvature with opposite signs in the two valleys, an in-plane electric field induces a Valley Hall Effect (VHE) for the carriers (**Figure 3**).[19] Note that the Berry curvature in the valence band is equal to that in the conduction band but with opposite sign.

The orbital magnetic moment has identical values in the valence and conduction bands

$$\boldsymbol{m}(k) = -\hat{z}\frac{2a^2t^2\Delta}{4a^2t^2k^2 + \Delta^2}\frac{e}{2\hbar}\tau_z \tag{10}$$

Nonzero $\boldsymbol{m}$ implies that the valleys have contrasting magnetic moments (through $\tau_z = \pm 1$) and thus it is possible to detect valley polarization through a magnetic signature. The orbital magnetic moment also gives rise to the circularly polarized optical selection rules for interband transitions. The Berry curvature, orbital magnetic moment, and optical circular dichroism $\eta(\boldsymbol{k})$ are related by

$$\eta(\boldsymbol{k}) = -\frac{\boldsymbol{m}(\boldsymbol{k})\cdot\hat{\boldsymbol{z}}}{\mu_B^*(\boldsymbol{k})} = -\frac{\boldsymbol{\Omega}(\boldsymbol{k})\cdot\hat{\boldsymbol{z}}}{\mu_B^*(\boldsymbol{k})}\frac{e}{2\hbar}\Delta(\boldsymbol{k}) \tag{11}$$

where $\mu_B^* = e\hbar/2m^*$ and $\Delta(\boldsymbol{k}) = (4a^2t^2k^2 + \Delta^2)^{1/2}$ is the direct transition energy, or band gap, at $\boldsymbol{k}$. At the energetic minima of the K and K' points we have full selectivity with $\eta(\boldsymbol{k}) = -\tau_z$. The transition at K couples only to σ^+ light and the transition at K' couples only to σ^-. This selectivity allows the optical preparation, control, and detection of valley polarization (**Figure 4**).

In summary, if the Berry curvature has different values at the K and K' points one can expect different particle behavior in each valley as a function of an applied electric field. If the orbital magnetic moment has different values at the K and K' points one can expect different behavior in each valley as a function of an applied magnetic field. Contrasting values of $\boldsymbol{\Omega}$ and $\boldsymbol{m}$ at the K and K' points give rise to optical circular dichroism between the two valleys, which allows selective excitation by photons with right or left helicity. In order to have contrasting values of $\boldsymbol{\Omega}$ and $\boldsymbol{m}$ while maintaining time-reversal symmetry, it is necessary that the material exhibit a lack of spatial inversion symmetry. Though spatial inversion symmetry can be induced in gapped graphene, for example, by biasing the substrate underlying bilayer graphene, monolayer 2D transition metal dichalcogenides meet this requirement without the need to externally introduce a band gap or symmetry breaking, and thus TMDs appear to be the most promising candidates for useful valleytronic applications.

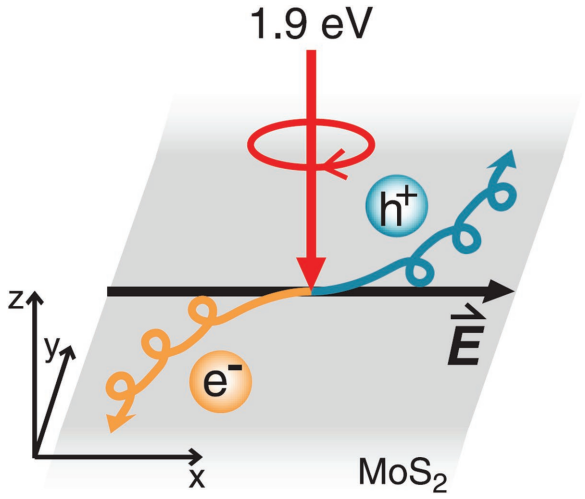

Figure 3. Anomalous motion perpendicular to an applied magnetic field (Valley Hall Effect) caused by finite and contrasting Berry curvature. Reproduced with permission.[19] Copyright 2014, AAAS.

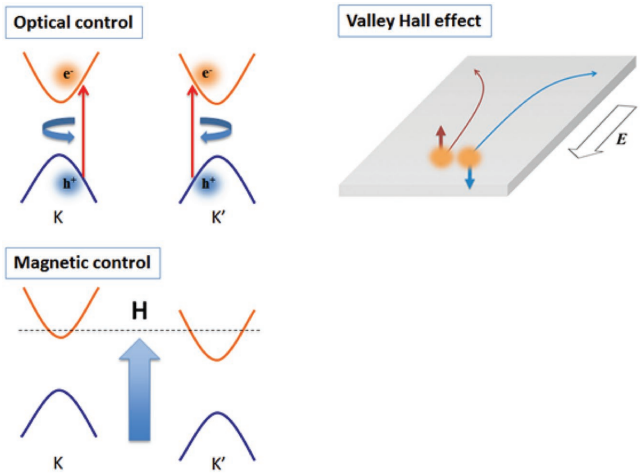

Figure 4. Three methods of control of the valley state: optical, electrostatic, and magnetic. Reproduced with permission.[52] Copyright 2017, the authors.

3. Emerging Opportunities and Technical Challenges

The focus of the valleytronics research community thus far has been on material growth, characterization, and valley physics experimentation. There has been limited consideration of practical devices or systems, which would exploit valleytronic properties. Thus it was important to devote time in the Workshop to discussion of the most promising applications for valleytronics and what are the greater technical challenges to realize these applications. Those useful technology implications are presented in this section.

3.1. Quantum Computing

Using TMDs as qubits for quantum computing has some very attractive potential benefits. It may be significantly easier to integrate thousands or millions of valley qubits on a layer of TMD in a simple planar architecture as compared to other modalities such as trapped ions. Because spin–orbit coupling provides energy separation between spin-up and spin-down states, and the valley index provides momentum separation between K and K' states, each quantum index provides a degree of protection of the other index. So spin protection of valley or valley protection of spin may provide a more favorable gate to coherence time ratio than unprotected qubit candidates. Because valley qubits are interrogated at optical frequencies, single qubits could be addressed through submicrometer waveguides allowing a higher density of qubit packing compared to that for superconducting qubits, which are limited by microwave transmission lines and inductors. Gate operation times may be concurrently faster as well.

On the other hand, there is the notable concern that large spin–orbit coupling will increase the interactions between the valley qubit and its environment, thus reducing coherence time. It is also important to note that entanglement between two valley qubits has not yet been demonstrated, and it is possible that the large separation in momentum space between the K and K' valleys may make entanglement difficult to realize.

In principle one could perform quantum gate operations on the valley pseudospin of excitons, electrons, or holes. As described below, there are tradeoffs between the lifetime and the ease of performing quantum operations with each of these species. It is not clear at this time which particle is the preferred storage medium for quantum information. Note that the quantum basis need not be composed of just a single particle, say an exciton, in state $|K\rangle$ or $|K'\rangle$. One could for example, employ two entangled excitons with a controlled coupling between them using singlet = $\frac{1}{\sqrt{2}}(|KK'\rangle - |K'K\rangle)$ and triplet = $\frac{1}{\sqrt{2}}(|KK'\rangle + |K'K\rangle)$ states as the basis.

For electrons and holes, the real spin is also available and one could conceive of a more complicated basis set comprised of $[|\uparrow_K\rangle,|\uparrow_{-K}\rangle, |\downarrow_K\rangle,|\downarrow_{-K}\rangle]$, which may hold some computational advantage. However it is appropriate to state that the spin/valley coupling that "protects" the spin or valley state is somewhat at odds with claiming there are two independent degrees of freedom in this system, as one spin state is lower energy than the other in each valley. At the same time one should recognize that spin and valley are not truly locked; the observation of a B exciton peak that exhibits similar photoluminescence polarization as the A exciton shows that to some extent one can initialize valley polarized populations of either spin state.[17]

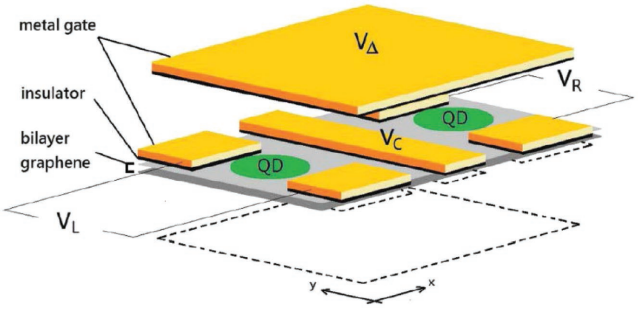

Figure 5. Proposed Valley qubit. Reproduced with permission.[20] Copyright 2013, American Physical Society.

A valley qubit architecture composed of two graphene quantum dots has been proposed (**Figure 5**).[20] The orientation of the valley pseudospin in each quantum dot places the qubit into a singlet or triplet state. The pseudospin in each quantum dot is rotated by an in-plane electric field between two parallel gates, and a control gate between the two quantum dots controls the coupling between them. The qubit can rotate from "North" to "South" on the Bloch sphere by changing the direction of an individual pseudospin, and motion around the equator is effected by allowing tunneling or an exchange interaction between the two quantum dots modulated by a control gate.

3.2. Classical Computing

Classical computational logic today is dominated by the silicon MOSFET. Metal oxide semiconductor field effect transistors (MOSFETs) are fundamentally limited by the Fermi–Dirac distribution of charge carriers in the source—carriers must have sufficient energy to traverse the energy barrier between the source and channel, where the barrier itself is controlled by a gate voltage. The number of carriers that have enough energy to do so is given by the tail of the Fermi–Dirac distribution function for the source. The effectiveness of the gate voltage in modulating the channel current is constrained thermodynamically, with no more than one decade of current increase per 60 mV of gate voltage at room temperature. This limits voltage scaling and thus power dissipation of the devices. State-of-the art 14 nm transistors operate at a drain–source voltage of 0.7 V; assuming a desired on/off current ratio of at least 10^6 the minimum possible operating voltage would be 0.36 V, though due to process variations and necessary operating margin 0.5 V is a more practical end-of-the-roadmap operating voltage. Scaling voltage and energy dissipation lower requires new device physics.

In valleytronic devices, where the manipulation of topological currents and opto-electronic effects can be used, this limit may very well be overcome since different physical phenomena are involved. One can speculate that the switching energy of a valleytronic information processing device would be on the

order of the valley splitting, which is a tunable quantity. The valley splitting must be chosen to be large enough to avoid thermal noise, but small enough to maintain a power advantage over conventional silicon MOSFETs. In cryogenic operation a 10 meV splitting may be sufficient but for room temperature operation 100 meV may be necessary [note that 10 meV energy splitting has been experimentally achieved,[21] but 100 meV has not]. If the control gate of a valley filter operates with a 100 mV swing, this would still translate to a 25× reduction in power since the switching energy scales quadratically with voltage.

It should be emphasized that valleytronics is not another subtle variation of spintronics. The physics underlying spin-based and valley-based computing are completely different. Most proposed spintronic devices require conventional charge transport for switching operations, though with some enhancement of their retention or on/off ratio characteristics provided by a conductivity difference between spin-up and spin-down electrons through a magnetic material. Spintronic devices have yet to demonstrate meaningful power or performance advantage compared to conventional silicon complementary metal oxide semiconductor (CMOS), technology as the thermodynamic switching limitations are similar. Valleytronic switches, by contrast, take advantage of unique light–matter interactions and/or evolution of the phase difference between particles in the *K* and *K′* valleys.

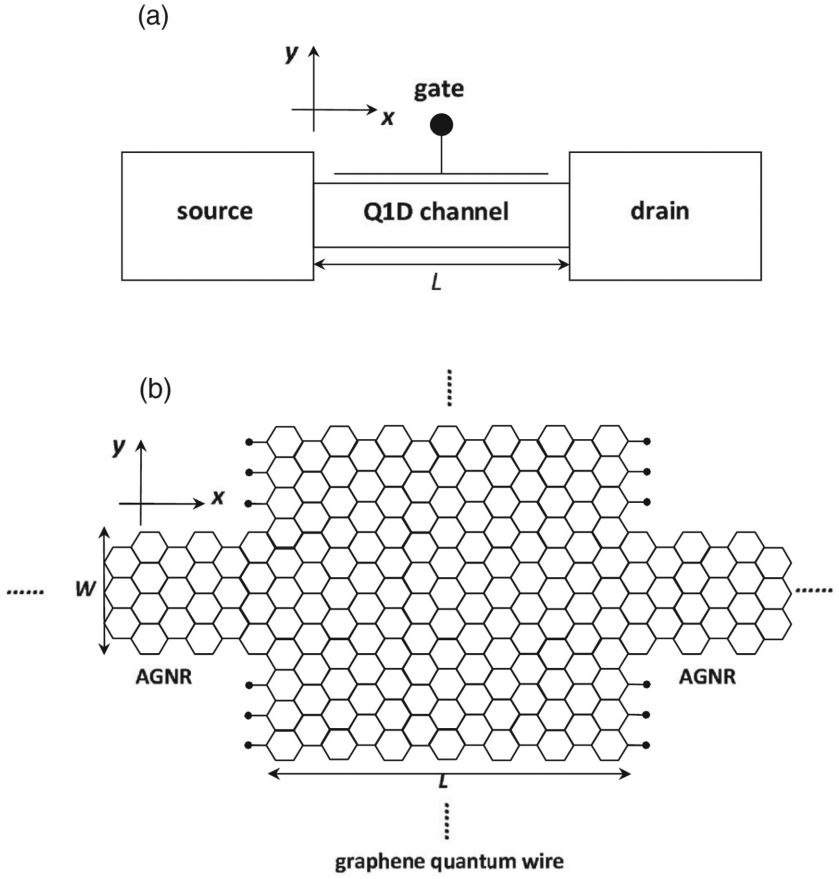

Figure 6. Concept for a valleytronic transistor based on the evolution of the phase of the K and K′ states between the source and drain. a) a three-terminal valley transistor device, where the source and drain are armchair graphene nanoribbons which inject and detect electrons in a specific polarization and the channel is a quantum wire of gapped graphene, b) graphene crystal structure of the device, with the channel region being subject to a lateral confinement potential in order to form a Q1D channel, and the zigzag edges of this section being passivated for stabilization. Reproduced with permission.[23] Copyright 2012, American Physical Society.

Though an all-valleytronic computational element is perhaps the most forward-thinking opportunity, one must also consider how valleytronics can enhance existing computational devices. By taking advantage of spin–orbit coupling, for example, valleytronic components may make spin-logic devices more attractive. Existing spin-logic device concepts require magnetic fields or relatively large currents to switch from an "on" to an "off" state. Because of this, spin-logic devices are either slow, power-hungry, or both. Thus in spite of determined effort over the past two decades, spin-logic devices are not widely seen as viable replacements for silicon CMOS. But by coupling spin-logic architectures with valleytronic materials it may be possible to eliminate the need for magnetic fields or large currents. If spin-polarized currents of either polarity can be efficiently generated in the valleytronic material, the spintronic material could be used as a static filter. The switching energy and switching speed would be governed by the operations on the valleytronic material. Note that valley-protection of spin could increase the spin lifetime and mean free path that are important for information storage and transport.

Alternatively, one could envision a heterogeneous valley/spin architecture. Valleytronics may provide a faster or lower power switch than silicon, but there is currently no proposal for how to make a valleytronic memory element. If we could transfer information between the spin and valley domains, and maintain the fidelity of that information across different material interfaces, we may be able to create a heterogeneous integration of valleytronics and spintronics which combines energy efficient switching with nonvolatile memory.

A valleytronic switch concept using a graphene nanoribbon approach is shown in **Figure 6**.[22] This device uses the Rashba effect to induce a phase difference between the electron wavefunctions in the *K* and *K′* valleys. Though the proposed device employed graphene, TMDs may be more advantageous. Another approach is to use engineered defects as part of a valley-filter device. At a line defect, it has been shown that asymmetric wavefunctions in these materials go to zero, so the density of states goes to zero and thus transmission equals zero. By contrast, for symmetric states transmission is 1. Therefore valley polarization could be induced by using line defects as a filter.[23] Alternatively, line defects could be used as physical barriers to confine valley transport between two parallel defects. Valley-polarized currents have been demonstrated in

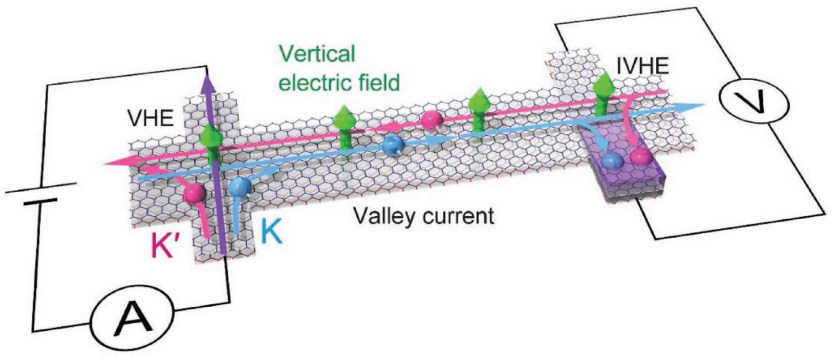

Figure 7. Device for valley polarized current transport. Reproduced with permission.[24] Copyright 2015, Springer Nature.

Hall-bar structures (**Figure 7**).[24] Integration of such a valley-polarized current source with valley-FETs, valley-filters, or spintronic elements will start to build the device toolbox necessary to generate logic gates. In addition, by finding ways to extend the length of these valley-polarized currents through improved material quality, valley amplifiers, or other means, one can then start to build valley-interconnects between devices.

In order to perform Boolean logic as it is done today, it is required that the electronic devices be cascaded. In a valleytronic architecture that implies there must be some element that provides valley current gain. To our knowledge there is no proposed valley device capable of gain, which is a critical technology gap.

3.3. Integrated Photonics Applications

A third device technology area is microphotonic elements. Optoelectronic devices may be more fault-tolerant than the computational elements described above; which is important as in the near term, devices built on monolayer 2D materials will have to contend with grain boundaries and other defects. The unique light–matter interaction in valleytronic TMDs could be a natural fit for development of microscale nonreciprocal optics, circularly polarized light emitters, and polarization sensitive detectors.

The first possible application for integrated polarization-sensitive photonic elements is the most common protocol for quantum communication, Quantum Key Distribution (QKD), which relies upon the generation of polarized photons and the remote detection of that polarization state. At the laboratory scale polarization light emission and detection can of course be achieved with conventional discrete optical components. But photon polarization and detection of the polarization state is decidedly more difficult at the integrated photonics scale. If these optical systems were scaled down to the microchip level, the societal benefit could be enormous, as one could provide secure quantum channels between everyday personal devices such as smart phones, tablets, and health monitoring devices. Valleytronics may be a practical route to chip-scale integration of QKD, as the monolayer TMD materials naturally produce light or left and right-circular polarization, and they can act as detectors of the same. By switching information from the photon to valley domains, one may be able to develop a quantum memory element or quantum repeater for long distance communications. Additionally, one can envision valleytronic single photon emitters that dynamically switch polarization based on electrical inputs. The fidelity of polarized light emission and improvements in quantum efficiency are technical challenges to be addressed.

A second opportunity exists in the development of valleytronic-based integrated optical isolators. Optical isolators are a long-awaited missing component in the integrated photonics toolbox. The inherent optical dichroism of valleytronic materials along with the means to address individual valleys through breaking time-reversal symmetry suggests that these materials could be ideally suited to form a microphotonic optical isolator. It may even be possible to construct a gated isolator that switches direction based on the handedness of a valley current.

Finally, one could also take advantage of the optoelectronic properties of valleytronic materials to make microscale polarization sensitive detectors for imaging applications, which would enable polarization sensitive focal plane arrays. Polarization sensitive optical detection can provide significant operational advantages, including differentiating man-made objects from natural background clutter and generating high-resolution 3D reconstructions from limited data. Full-Stokes polarimeters measure all four components of the Stokes vector, allowing reconstruction of the polarization of the incoming light whether it is circular, linear, or elliptical. Full-Stokes polarimeters have been demonstrated using mechanically rotated optical filters and liquid crystal-based variable retarders. However, these systems are slow to rotate between different polarizations, which causes loss of resolution due to scene movement between image captures. An intrinsically polarization-sensitive detector capable of operating at fast frame rates with no moving parts would open new capabilities for space-based imaging and ranging as well as terrestrial applications. But there are no commercial photodetectors that are inherently capable of discriminating between left, right, and linearly polarized light, as would be possible with detectors made from valleytronic materials.

4. Valleytronic Properties

In this section we discuss four essential valleytronic elements: valley lifetime, valley coherence, valley manipulation, and valley transport. We define valleytronic quality material as material that possesses the combination of lifetime, coherence time, and mean free path to perform useful valleytronic functions. The current state of the art is presented as well as the gap between the existing valleytronic properties and those needed for useful devices.

4.1. Valley Lifetime and Coherence

Valley lifetime and coherence are critically important to useful information processing applications, as devices relying upon polarized valley populations are only useful for as long as that valley polarization persists. Here we use "valley lifetime" to mean how long a population of particles remains in the K or K'

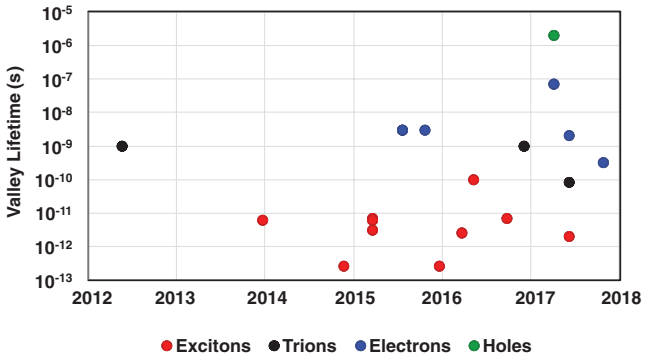

Figure 8. Valley polarization lifetime as a function of publication year for excitons, trions, electrons, and holes in various monolayer TMDs.

valley before scattering to the opposite valley and "valley coherence" is reserved for discussing the phase relationship between a particle in a superposition of two different valleys, such as that induced by linearly polarized light.[25]

Figure 8 shows the valley lifetime of electrons, holes, excitons, and trions (excitons with an extra electron or hole), across several different TMDs as measured by circularly polarized photoluminescence and Kerr rotation techniques by various research groups.[17,26–42] Most of these data were taken at low temperature (≈4 *K*). Details are available in the references. The valley lifetime can be shorter or longer than the recombination lifetime of the particle. If the valley lifetime is long compared to the recombination lifetime, near-unity valley polarization of the emitted photoluminescence is expected. If the valley lifetime is short compared to the recombination lifetime, a small polarization signal is expected. For practical applications both the valley lifetime and the recombination lifetime need to be as long as possible, and so from this perspective electrons and holes may prove more useful than excitons or trions.

Compared to valley lifetime, exciton valley coherence time has been scarcely considered in the literature. Though coherence has been observed through linearly polarized photoluminescence, we are aware of only two published measurements of valley coherence time.[37,43] These suggest an exciton valley coherence time of less than 1 ps. It is reasonable to expect that valley coherence time will be equal to or shorter than valley lifetime just as T_2 is typically less than T_1 in spin systems.

Coherence times of picoseconds to microseconds may not appear promising. Though long absolute coherence times may be preferable, what is essential is that the coherence time be long compared to the gate operation time. For nanosecond gate operations, microsecond coherence time may be sufficient. Unfortunately we do not yet have solid experimental data on the time to perform a gate operation. Theoretically, the minimum time for a single qubit gate operation is given by

$$t = \hbar \frac{\Delta E}{\Delta \phi} \tag{12}$$

where ΔE is the energy separation between the two valley states and $\Delta\phi$ is the desired phase gate. For an 18 meV energy splitting[21] a $\pi/2$ gate could in theory be implemented in 54 fs, though in practice gate fidelity will degrade considerably at such a fast gate speed. Experimental demonstrations of gate operations are necessary to make an accurate assessment.

4.1.1. Excitons

Valley lifetime for excitons in monolayer 2D TMDs is quite short, ranging from 0.1 to 100 ps across different TMDs and experimental conditions. The exciton recombination lifetime is longer in these materials, about 10 ps. Depending on the experiment, the valley lifetime can be longer or shorter than the recombination lifetime, which partially explains why measured photoluminescence polarization varies from nearly 100% to only a few percent in different reports.

The dominant mechanism for loss of valley polarization is not firmly established. One theory is that the loss is dominated by the exciton exchange interaction where annihilation of an exciton in one valley is accompanied by the formation of an exciton in the opposite valley. If true, it may be very difficult to construct a useful device based on simple excitons as it is not clear that there is any practical way to discourage this exchange interaction and prolong valley lifetime.

There is evidence that dark exciton valley lifetimes may be much longer, on the order of hundreds of picoseconds. Dark excitons are bound electron–hole pairs where the electron and hole have equal spin. This situation can occur when splitting of the conduction band by spin–orbit coupling is more pronounced, and the valence band maximum is of opposite spin to the conduction band minimum. Typically, if a spin-up electron is promoted to the conduction band, it leaves behind a spin-down hole thus preserving spin conservation. If conduction band splitting is large, and the spin-down state is lower, it would be energetically favorable for the spin-up electron to relax to the lowest conduction band even though that would entail a spin flip. One is left with a spin-down electron and a spin-down hole. Since exciton recombination is spin-forbidden in this case, photoluminescence is not observed and the exciton is termed "dark." In MoX_2 TMDs the conduction band splitting is quite small, and thus both the upper and lower conduction bands will be populated, and bright exciton effects will be seen. In WX_2 TMDs the conduction band splitting is on the order of 30 meV, and at low temperature dark exciton populations may dominate the physics. In addition to the long dark exciton recombination lifetime, since the exciton exchange interaction is forbidden for dark excitons the dark exciton valley lifetime is longer as well. Coherent superposition or manipulation of dark excitons is more difficult to observe and has not yet been experimentally demonstrated.

Indirect or interlayer excitons, where the hole is in one layer and the electron is in the other layer of a heterogeneous bilayer stack of 2D materials, exhibit much longer lifetimes, on the order of 100 ns. Similar to the argument above for dark excitons, it is conjectured that indirect excitons are protected against the exchange interaction. Indirect excitons have the advantage of being bright as opposed to dark, that is to say the oscillator strength is large, and they are much more easily seen in photoluminescence experiments and presumably are easier to manipulate with light as well.

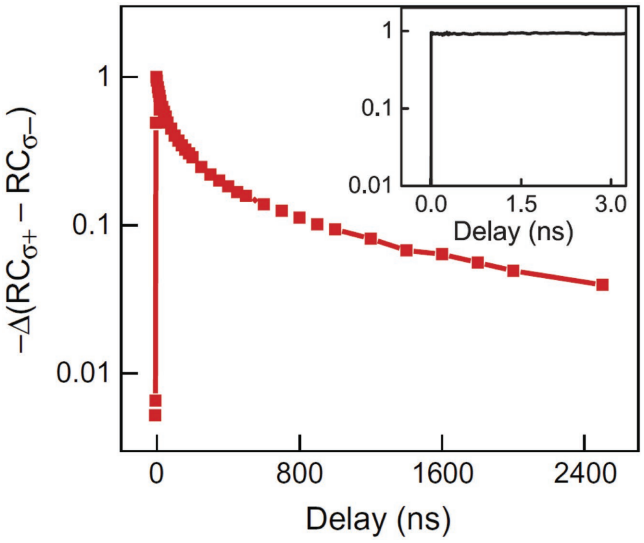

Figure 9. Decay dynamics of the resonant circular dichroism signal from a WS_2/WSe_2 heterostructure at 10 K. No decay is observed within 3.5 ns (inset). The decay curve over a longer time scale shows a significant slow decay component with a lifetime of more than 1 ms. Reproduced with permission.[53] Copyright 2017, AAAS.

But again, coherent superposition and manipulation of indirect excitons are open questions at this time.

Can one increase valley lifetime yet further? In cases where valley lifetime is determined by some extrinsic factor (as opposed to the exchange interaction) there is the potential to mitigate the loss mechanisms. For example, if scattering off impurities or defects is the dominant mechanism in loss of valley polarization, it should be possible to increase valley lifetime by reducing defect density. The effect of phonons, disorder, and nuclear spins on valley lifetime has not yet been the subject of study. Though speculative, if the valleytronic material is patterned into 1D nanowires or 0D dots with critical dimensions on the order of nanometers, quantum confinement may reduce loss mechanisms and increase valley lifetime.

4.1.2. Electrons, Holes, and Trions

Although data are scarcer than for excitons, valley lifetimes for charged carriers have been measured and appear to be much longer than for excitons: 0.1–1 ns for trions, 1–100 ns for electrons, and as long as 2 µs for holes (**Figure 9**). It is believed that the lifetime is shorter for electrons than for holes because the smaller spin–orbit coupling in the conduction band results in less spin-protection of the valley state. It is likely that electron and hole valley lifetimes are much longer than for excitons because the exchange interaction is not available for free carriers. Additionally, the recombination lifetime of free carriers should be long compared to that of strongly bound excitons. Still, electron and hole depolarization mechanisms must be understood to maximize free carrier valley lifetime.

There has been no measurement of valley coherence of electrons or holes. Relative to the valley lifetime, the coherence time is expected to be small as crystal momentum is a continuous variable, and any small perturbation of an electron or hole from the minimum energy state may destroy coherence. Excitons, by contrast, exhibit one tightly bound state for each region in momentum space. Thus excitons have the advantage of demonstrated coherence, but electrons and holes have the advantage of longer valley lifetime. Further investigations are necessary to determine which species is better suited for valleytronic applications.

4.2. Valley Manipulation

To be of practical value, one must be able to perform a manipulation of the valley state within its lifetime. Though it is known how to create a valley exciton state at any point on the Bloch sphere using circular, linear, or elliptically polarized light, it is not clear how one can perform an arbitrary rotation from one state to any other state on the sphere. Manipulations have been shown in limited cases.[37,43] Using linearly polarized light one can create a superposition state $\frac{1}{\sqrt{2}}(|K\rangle + e^{-i\omega t}|K'\rangle)$ on the equator of the sphere, where ω is proportional to the energy difference been the two valleys. Breaking the degeneracy between the K and K' states by DC magnetic or AC electric fields will cause the phase to evolve differently in the two states, thus effecting motion along the equator (**Figure 10**). By contrast, rotating a state in the orthogonal direction, that is to say a π rotation from one pole to another, has yet to be realized. Demonstrating arbitrary valley state rotations and developing valley analogs of NMR and spin echo techniques are necessary steps toward systems that exploit controlled valley manipulation.

The measured Zeeman splitting of excitons in these materials is very weak, about 0.2 meV T^{-1}. This means extremely high DC magnetic fields would be necessary to perform a state rotation within the valley coherence time. However, it has been shown that breaking of time-reversal symmetry through the optical Stark

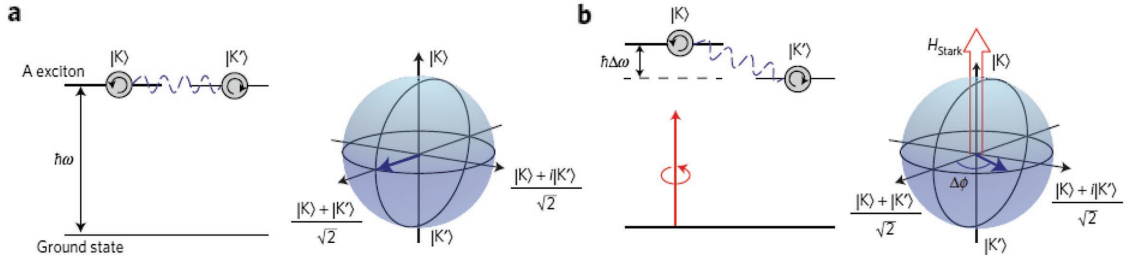

Figure 10. Representations of the Valley state on the Bloch sphere. a) A coherent superposition of K and K' states, b) Lifting the degeneracy between states induces motion of the state around the equator. Reproduced with permission.[43] Copyright 2017, Springer Nature.

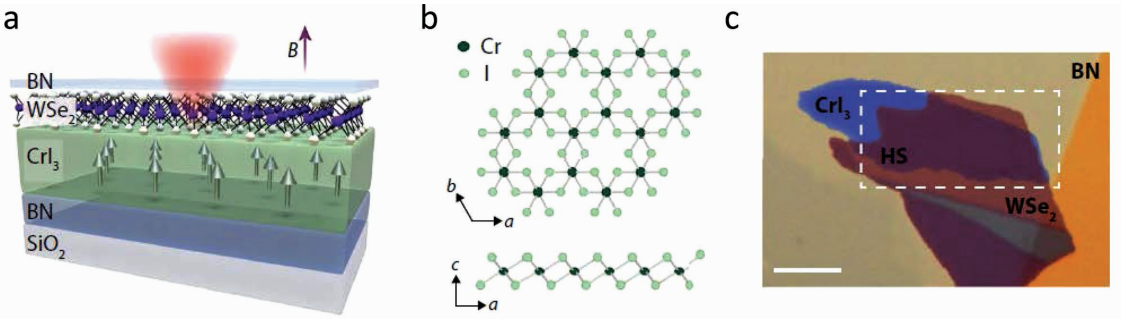

Figure 11. Heterostructure of WSe_2 on CrI_3. a) Schematic of van der Waals heterostructure formed by monolayer WSe_2 and ferromagnetic-layered semiconductor CrI_3 and encapsulated by h-BN. b) Top and side views of CrI_3 crystal structure. c) Optical microscope image of device Scale bar, 5 µm. Reproduced under the terms and conditions of the Creative Commons Attribution NonCommercial License 4.0.[45] Copyright 2017, the authors, published by AAAS.

effect (which can induce an effective magnetic field of at least 60 T) can be observed without any applied magnetic fields.[21] If creative methods can be developed to increase the effective exciton dipole moment, this effect will be even more pronounced. Additionally, heterostructures of semiconducting TMDs on top of magnetic materials have demonstrated impressive Zeeman splitting through the magnetic proximity effect, such as with WSe_2 on EuS[44] or CrI_3 (see **Figure 11**).[45] Other options for creative means to break time-reversal symmetry should be explored, as robust low-power mechanisms for valley splitting will be necessary to build practical information processing elements.

4.3. Valley Transport

For valleytronics to be useful, we must also transport valley information across a crystalline domain, across domain boundaries, and perhaps between different materials. Since excitons are neutral species we cannot control their motion by applied fields. Alternatively, transferring valley information from excitons to charged carriers to satisfy both valley manipulations and transport needs may be required. Converting valley information into the optical domain—that is, from the exciton, electron, or hole into a photon with the corresponding chirality—may be another route to accomplish efficient valley transport.

TMDs may not be ideal for information transport, due to their low mobility. But this could be circumvented by using graphene interconnects if one can solve the problem of transferring valley information between the two materials. If one could transfer valley information directly from TMDs into graphene, one could use the best material for switching (TMDs) and transport (graphene). The first examples of valley transfer between different materials have recently been demonstrated.[46,47]

Measurement of valley mean free path and the causes of valley information scattering in real space is essential to understand the practical limits of valley information transport. These may require more sophisticated pump–probe experiments with spatially delocalized pump and probe beams.

4.4. Other Valley Phenomena

We note that there are a number of other interesting areas of valley physics that have not been explored in depth. For example, though superconductivity in 2D materials has been demonstrated, valley-polarized superconductivity has not been addressed. Normally Cooper pairs would consist of electrons from opposite valleys, but in valleytronic materials the Cooper pairing may be quite unusual. Is it possible to create a new superconducting quasiparticle with electrons from the same valley? 2D superconductivity at low electron density as well as superconductivity in Landau Levels has not yet been studied. Valley polarized supercurrents may have application in cryogenic single flux quantum information processing, possibly as a means of information storage in that technology. Or perhaps a valley-polarized supercurrent will allow a new degree of freedom in superconducting artificial atom qubit architectures.

In valleytronic materials, the broken inversion symmetry allows topological currents to propagate along edge modes perpendicular to an applied electric field. There is no net current flow (K and K' currents are counter propagating) and the process is dissipationless. It may be possible to exploit these currents for dissipationless valley information transport.

While spin-lasers in conventional semiconductors such as GaAs have been explored, spin-lasers employing valley polarized states in TMDs may be more efficient due to longer hole spin lifetime in MoS_2 as a result of the valley protection of the spin state.[48]

Finally, it should be noted that valleys other than K/K' do exist in hexagonal 2D materials, such as at the Γ and Q/Q' points. Though these valleys do not represent global energetic minima, one should investigate if there are persistent valleytronic effects at these points.

5. Valleytronic Material Growth and Device Processing Challenges

5.1. Domain Size and Grain Boundaries

Valleytronic properties are predicated upon the solid-state physics of an ideal single crystal. By contrast, an amorphous film of MoS_2 presumably will not exhibit any useful valleytronic effect. In the absence of data to the contrary, we assume that ideal valleytronic effects will be observed only if the entire active area of the device or circuit is composed of a single crystalline domain. Polycrystalline material may exhibit some degree of valleytronic behavior within each small

crystalline domain, but valleytronic information will likely be lost if the macroscopic area of the device is comprised of multiple small domains with different orientations. Valley information transport across a disordered grain boundary may be inefficient or even impossible.

So how does one address this issue? Ideally by having a single crystalline domain across an entire substrate as is the case with commercial electronic products fabricated on single-crystal wafers (e.g., Si, SiGe, GaAs, GaN, SiC, or InP). With bulk materials such as these conventional semiconductors, essentially perfect crystallinity across a wide area is readily achieved by growth from a melt or by homoepitaxy. Unfortunately, it is not currently possible to grow a large single monolayer of MoS_2 (or any TMD) from a melt, and homoepitaxy is not consistent with isolating a monolayer. High-quality single-crystal films of bulk semiconductors can also be grown through heteroepitaxy, though it requires a succession of strain release layers to gradually improve the lattice matching between the substrate and the desired material. It appears upon initial inspection that large-area single-crystal TMD growth could be performed in the same way. However, it is critical to keep in mind that valleytronic effects generally require "a single monolayer" of TMD. Heteroepitaxy of a bulk material, such as GaN, does not begin with an even surface coverage of a single atomic layer of material. Instead, the first few angstroms of GaN "puddle up" into islands that do not coalesce into a continuous film until a thickness of some nanometers is achieved. Fortunately, these islands register with the underlying strain-relief layer, so as the material grows thicker these early-growth domain boundaries disappear and one is eventually left with a uniform single-crystal film. But clearly this approach will not work when a single monolayer is needed.

This is a significant problem. There is a large literature on growing monolayer TMDs by vapor phase transport (VPT), vapor phase epitaxy, chemical vapor deposition (CVD), atomic layer deposition, and molecular beam epitaxy on different substrates including silicon, silicon dioxide, sapphire, graphene, and hexagonal boron nitride (hBN). All of these approaches essentially try to perform monolayer heteroepitaxy and their results are broadly similar. Although large-area growth is frequently reported, the material is far from the wafer-sized single crystal that one might envision, instead domain sizes range from tens of nanometers to tens of micrometers. Frequently the material does not form a continuous film at all, but instead consists of a sparse scattering of isolated micrometer-sized single crystals. Indeed, one of the most time consuming parts of this work is to search across the sample for a "publication-worthy" flake upon which to perform spectroscopic analysis or device fabrication. In the cases where the film is continuous, the material is polycrystalline with domains that do not register with one another and are separated by highly disordered grain boundaries and overlapping bilayer regions. The existence of multiple domains can be seen, for example, in transmission electron micrograph (TEM) images of these samples (**Figure 12**). Increased particle scattering will occur as the number of domains and grain boundaries increases, resulting in loss of valley information.

Development of a synthesis technique for large (tens of mm) single-crystal domains of monolayer TMD material is essential

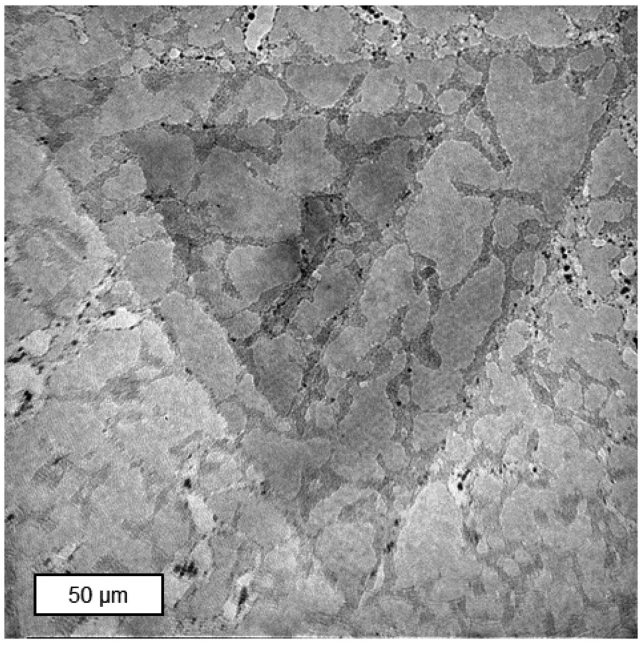

Figure 12. TEM image of WS_2 grown by vapor phase epitaxy on a sapphire substrate, revealing variation in domain sizes and multilayer growth.

for developing real systems that exploit valleytronic behavior. Projects to explore adapting conventional heteroepitaxy to monolayer TMD growth will provide valuable insight into whether it is feasible to grow large area single-crystal TMDs by this technique. Alternatively, one could explore increased domain size through homoepitaxy, for example, by growing on top of exfoliated flakes or bulk geological material, along with a means to cleanly separate the newly grown monolayer. Liquid phase synthesis should be considered as well. In the end, there may be fundamental or practical limitations to monolayer TMD domain size, such as the width of the atomic layer terraces of the underlying substrate. Theoretical study of the thermodynamics of monolayer TMD formation over these length scales may be very insightful.

5.2. Defects, Defect Reduction, and Doping of TMDs

Large single crystals of even common commercial materials are of course not defect-free, and in the case of valleytronic material random defects will be detrimental to the valleytronic properties. Useful devices will transport electrons, holes, or excitons from one spatial location to another without undue loss of valley information. This implies that valley mean free path or valley scattering length is important.

It is probable that vacancies, substitutions, and extended defects will all adversely affect valleytronic properties. The role of some donor defects such as chalcogen vacancies or excess metal atoms and some acceptor defects such as metal vacancies or excess chalcogen atoms have begun to be explored. Further studies of these and other defect types to understand the quantitative impact on valleytronic properties will be of great utility.

One then turns to defect reduction. Within the small domains of single-crystal TMD flakes described above, the

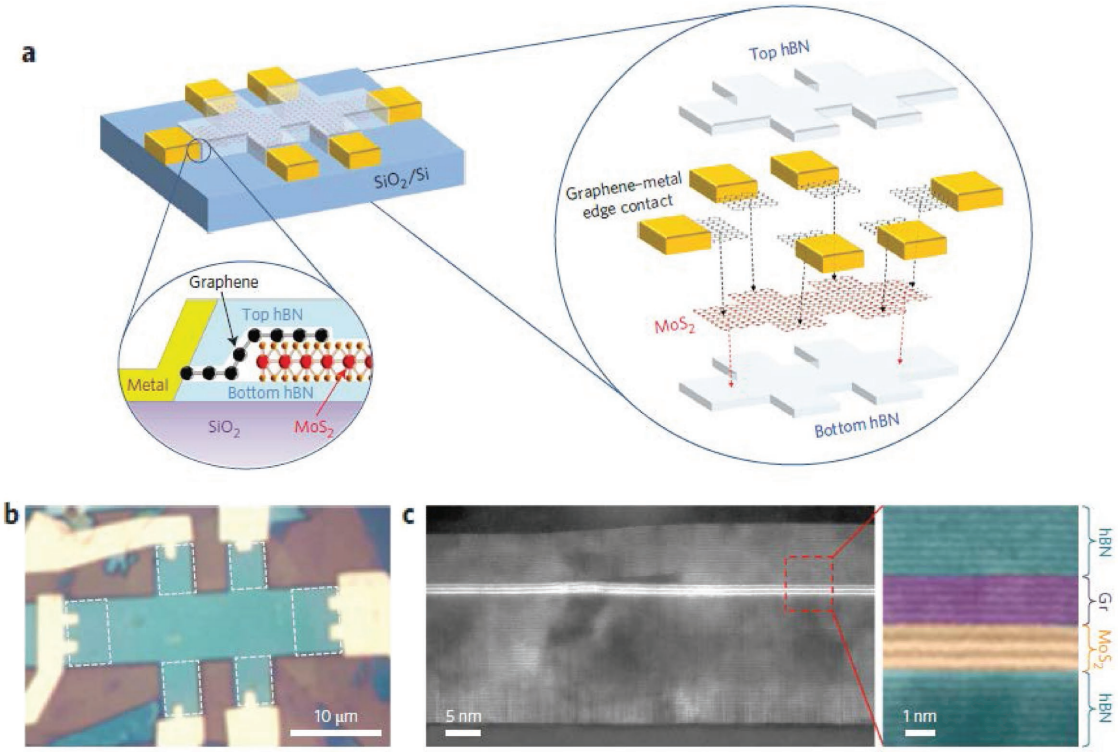

Figure 13. High mobility measurement of MoS_2 enabled by heterostructure formation. Reproduced with permission.[49] Copyright 2015, Springer Nature.

defect density of TMDs such as MoS_2 grown by VPT or CVD is about 10^{13} cm^{-2}. This is roughly 10 000 times higher than the defect density in microelectronic-grade silicon. Better understanding of the kinetics of TMD growth by various means should result in reduction of defect density. Defect healing of TMD material, such as by annealing of flakes in chalcogen or other ambient, followed by measurements of defect density and valleytronic properties should be pursued.

But what defect density is good enough? This cannot yet be definitively answered as we do not have a direct correlation between defect density and valleytronic properties, and we do not know the fault tolerance of valleytronic devices. It has been proposed that valley polarization is linearly proportional to the defect density for very high levels of defects, but that is likely an optimistic scenario when extrapolated to low defect densities. An effort to determine the thermodynamic limits of defect density, combined with the effect of those defects on valley lifetime and mean free path, would allow us to assess the realistic performance potential of valleytronic materials.

For devices that rely on charged particles, the dopant density in these materials must be tunable and well controlled. Currently, material grown in different laboratories exhibits widely varying dopant density. In some cases, a given TMD such as MoS_2 can even exhibit n-type or p-type behavior as a result of differences in sample preparation. It is likely that the substrate material, process cleanliness, and other subtle variables are important here. Maturation of growth processes and protocols is necessary to control dopants.

5.3. Device Processing

After growth of excellent valleytronic quality 2D material, one must process that material in to a useful device. This brings up challenges with respect to suitable substrate materials, clean interfaces, patterning methods, and electrical contacts.

Substrates such as silicon dioxide or sapphire have strong interactions with 2D materials. Some substrate materials are known to quench photoluminescence, or even attract adsorbed species that contribute to the observed quenching. By inserting low energy buffer layers such as hBN or graphene (**Figures 13** and **14**) between the TMD and the substrate, the material

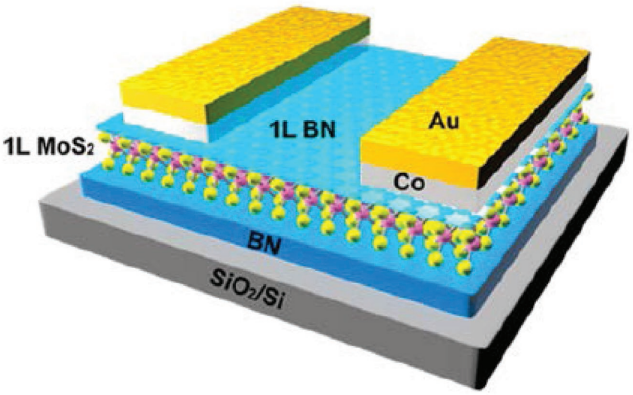

Figure 14. Complex metal stack required for good ohmic contact to MoS_2. Reproduced with permission.[50] Copyright 2017, American Chemical Society.

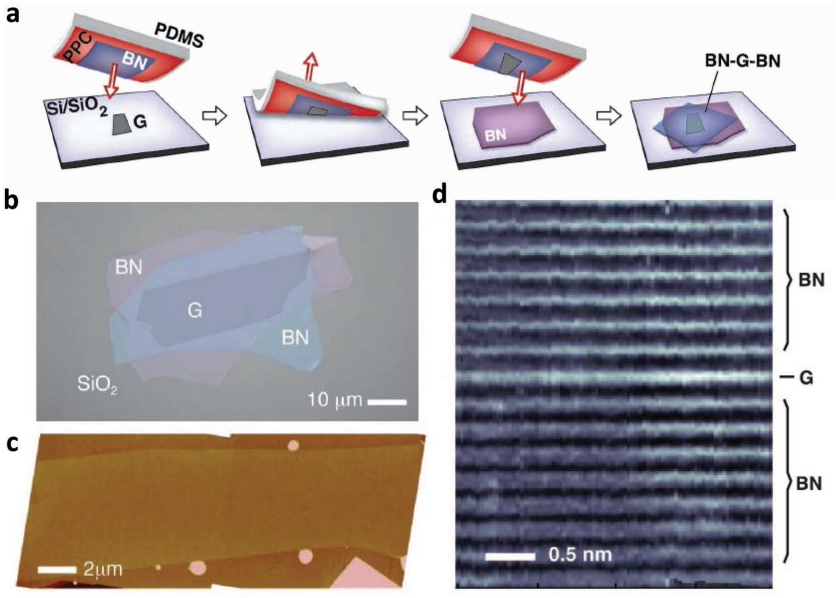

Figure 15. BN/graphene/BN heterostructures fabricated by stamping. a) Schematic of the assembly technique, b) optical image of a multilayered heterostructure using the process, c) AFM image of a large-area encapsulated graphene layer, d) high-resolution crosssection of the device. Reproduced with permission.[51] Copyright 2013, AAAS.

exhibits improved properties, such as higher mobility or increased indirect exciton lifetime, compared to simple single layer TMDs in direct contact with a bulk substrate.[49,50] The substrate surface can also affect the morphology and smoothness of the 2D films.

More generally one can say that interfaces are extremely important during 2D material device fabrication. Protecting the 2D material from environmental contamination by employing a multilayer sandwich (**Figure 15**) provides further improvement of valleytronic properties.[51] Current methods for multilayer stacking are time-intensive, labor-intensive, and low-yield. Simple and reproducible recipes for cleaning and preparing atomically sharp interfaces are desired.

The TMD materials must be patterned into useful geometries. **Figure 16** demonstrates that large patterns up to several hundreds of micrometers in size can be directly patterned into a TMD material using conventional optical lithography and etching techniques. This is significant as valleytronic circuits of moderate complexity will require patterning over domains of hundreds of micrometers, and potentially much larger. It should be noted that the effects of introducing undesired edge states and defects by patterning and etching the TMD can be disadvantageous to valleytronic properties. It has been suggested that virtual gate-defined edges produce better quality measurements than hard physical edges, but more work needs to be done on this topic.

Good electrical contact to the 2D TMD is a requirement for most device concepts. It has been shown that metal/TMD electrical contact quality is extremely sensitive to surface contamination. Contact resistance decreasing as one moves from typical vacuum, to high vacuum, and to ultrahigh vacuum metal deposition processes. Without due care, instead of low resistance ohmic contacts at the metal–semiconductor interface, Schottky barriers are formed that significantly alter the electronic behavior of devices.

5.4. Multilayer TMDs

This paper has almost exclusively considered monolayer 2D materials for valleytronics, since the spatial inversion symmetry is restored in bilayers and thus valleytronic properties are lost. However, in the presence of a substrate, an electric field, or a strain field, the inversion symmetry of a bilayer is broken again, and valleytronic behavior is (at least partially) restored. One could try to exploit this effect by applying an electric field across a bilayer material to turn valley currents on and off. For example, in a monolayer of TMD material, the conductivity due to the VHE cannot be easily tuned, and its magnitude is intrinsically linked to the doping level. It is difficult to turn on and off the VHE, as one would want do with a valleytronic switch. In bilayer TMDs, the VHE is absent as inversion symmetry is restored. However, electrostatic gating of bilayer TMDs induces some degree of symmetry breaking, in effect switching between a bilayer and two noninteracting monolayers. The strong dependence of both the magnitude and polarity of the Valley Hall conductivity on the applied field presents a way to electrically tune the VHE in bilayer TMDs, and thus bilayers of TMDs may be useful for selective valleytronic transport.

Bilayers of stacked 2D materials (**Figure 17**) provide an additional rotational degree of freedom to control valleytronic effects as well. The Moiré patterns in stacked TMD bilayers

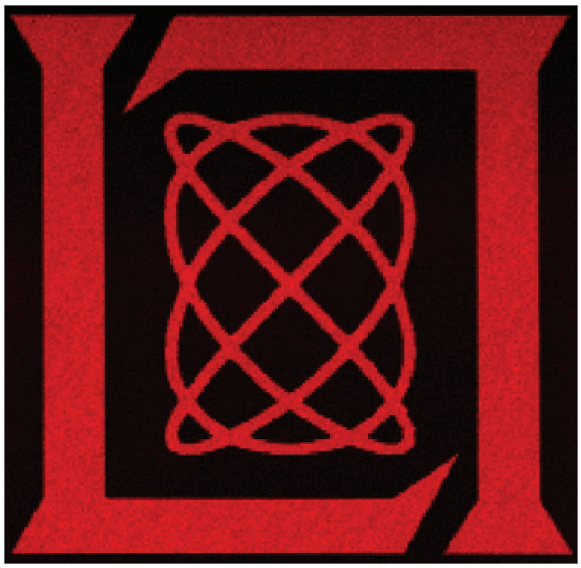

Figure 16. Raman image of the in-plane E_2g mode of tungsten disulfide grown by vapor phase epitaxy and patterned at a large-scale (figure is 400 μm on a side) using optical lithography and plasma etching.

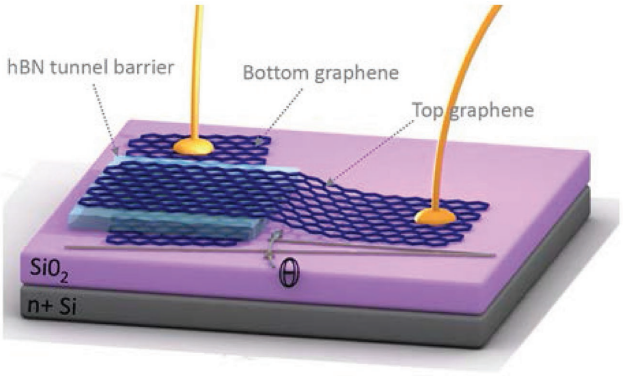

Figure 17. Twisted bilayers of graphene show valley-dependent effects based on the twist angle. Reproduced with permission.[54] Copyright 2014, Springer Nature.

produce periodic potential wells as deep as 160 meV. These may be useful for creating quasi-atomic lattices of particles that can be employed as arrays of devices for memory or logic operations. It is known that exciton-polaritons can condense into a Bose–Einstein condensate (BEC). If the BECs at given lattice points in the Moiré pattern can be made to interact, it may be possible to realize the BEC equivalent of an atom interferometer.

5.5. New Materials

The list of 2D materials continues to grow but from a valleytronics perspective, not all of these new 2D materials are clearly useful. 2D materials with improved valley lifetime and mean free path are certainly needed. Synthesis of such material by trial and error is likely to be very labor intensive, especially as one begins to consider binary and ternary alloys. A materials modeling effort to design the next generation of valleytronic material would be efficient. Basic questions remain unclear, such as: Will alloys of TMDs retain (or enhance) valleytronic properties? Can we design materials with significant spin splitting in the conduction band as well as the valence band? Or is valleytronics practical in another class of materials beyond 2D hexagonal honeycomb lattices? A concerted effort in computational materials design to optimize valleytronic properties would be beneficial, starting with TMDs and other van der Waals layered materials and extending to novel low-dimensional heterostructures such as oxides, nitrides, and mixed phases.

6. Summary and Outlook

The new physics associated with manipulation of the valley degree of freedom has the potential for transformative impact. Section 3 provides several ideas for valleytronic information processing and optoelectronic elements. At the same time, we assert that there have been no valleytronic device concepts yet published that convincingly promise performance advantages in practical systems. This is a critical gap in the argument for valleytronics as a technology element as opposed to an interesting physics phenomenon. In addition, we still need to demonstrate that valleytronic properties (valley lifetime, valley coherence time, and valley mean free path) are robust enough to perform useful functions. Whether valleytronic behavior is sufficiently retained at room temperature has profound implications for the class of applications for which valleytronics is suitable; robust valleytronic behavior at room temperature is still an open question.

It is commonly stated upon the discovery of a new material or physics phenomenon that it will enable new products and technologies. However very few new discoveries actually develop in to real products. To achieve real-world impact the integrated device needs to provide significant performance or power advantages over the existing technology, preferably at similar cost. This is a formidable challenge, and we have attempted to be quite realistic in our assessment of the potential impact of valleytronics. We have identified several areas in which the unique physics of valleytronic materials could meet this challenge.

We need to establish concrete device concepts, improve device processing, understand the structure–process–properties relationships of valleytronic materials, improve single-crystal growth, and demonstrate arbitrary rotations of the valley state around the Bloch sphere, among other things. The required research investment is significant and must be well coordinated. Meeting these challenges will require an interdisciplinary and convergent approach employing experts in materials science, solid state physics, device engineering, and computer science.

Acknowledgements

The Valleytronic Materials, Architectures, and Devices workshop was sponsored by the MIT Lincoln Laboratory Technology Office and by NSF. This material is based upon work supported by the Assistant Secretary of Defense for Research and Engineering under Air Force Contract No. FA8721-05-C-0002 and/or FA8702-15-D-0001. Any opinions, findings, conclusions, or recommendations expressed in this material are those of the author(s) and do not necessarily reflect the views of the Assistant Secretary of Defense for Research and Engineering. The authors thank Dimitris Pavlidis for his support and leadership of the Valleytronics Workshop, as well as for valuable comments on this manuscript.

Conflict of Interest

The authors declare no conflict of interest.

Keywords

quantum computing, valleytronic computing, valleytronics

Received: April 18, 2018
Revised: June 3, 2018
Published online:

[1] K. S. Novoselov, A. K. Geim, S. V. Morozov, D. Jiang, Y. Zhang, S. V. Dubonos, I. V. Grigorieva, A. A. Firsov, *Science* **2004**, *306*, 666.
[2] K. S. Novoselov, A. K. Geim, S. V. Morozov, D. Jiang, M. I. Katsnelson, I. V. Grigorieva, S. V. Dubonos, A. A. Firsov, *Nature* **2005**, *438*, 197.

[3] Y. Zhang, Y.-W. Tan, H. L. Stormer, P. Kim, *Nature* **2005**, *438*, 201.
[4] K. F. Mak, C. Lee, J. Hone, J. Shan, T. F. Heinz, *Phys. Rev. Lett.* **2010**, *105*, 136805.
[5] A. Splendiani, L. Sun, Y. Zhang, T. Li, J. Kim, C.-Y. Chim, G. Galli, F. Wang, *Nano Lett.* **2010**, *10*, 1271.
[6] D. L. Duong, S. J. Yun, Y. H. Lee, *ACS Nano* **2017**, *11*, 11803.
[7] K. F. Mak, J. Shan, *Nat. Photonics* **2016**, *10*, 216.
[8] S. Z. Butler, S. M. Hollen, L. Cao, Y. Cui, J. A. Gupta, H. R. Gutierrez, T. F. Heinz, S. S. Hong, J. Huang, A. F. Ismach, E. Johnston-Halperin, M. Kuno, V. V. Plashnitsa, R. D. Robinson, R. S. Ruoff, S. Salahuddin, J. Shan, L. Shi, M. G. Spencer, M. Terrones, W. Windl, J. E. Goldberger, *ACS Nano* **2013**, *7*, 2898.
[9] B. H. Nguyen, V. H. Nguyen, *Adv. Nat. Sci.: Nanosci. Nanotechnol.* **2016**, *7*, 043001.
[10] F. Liu, J. Zhou, C. Zhu, Z. Liu, *Adv. Funct. Mater.* **2017**, *27*, 1602404.
[11] W. Choi, N. Choudhary, G. H. Han, J. Park, D. Akinwande, Y. H. Lee, *Mater. Today* **2017**, *20*, 116.
[12] J. R. Schaibley, H. Yu, G. Clark, P. Rivera, J. S. Ross, K. L. Seyler, W. Yao, X. Xu, *Nat. Rev. Mater.* **2016**, *1*, 16055.
[13] X. Xu, W. Yao, D. Xiao, T. F. Heinz, *Nat. Phys.* **2014**, *10*, 343.
[14] D. Xiao, G.-B. Liu, W. Feng, X. Xu, W. Yao, *Phys. Rev. Lett.* **2012**, *108*, 196802.
[15] D. Xiao, W. Yao, Q. Niu, *Phys. Rev. Lett.* **2007**, *99*, 236809.
[16] T. Cao, G. Wang, W. Han, H. Ye, C. Zhu, J. Shi, Q. Niu, P. Tan, E. Wang, B. Liu, J. Feng, *Nat. Commun.* **2012**, *3*, 887.
[17] K. F. Mak, K. He, J. Shan, T. F. Heinz, *Nat. Nanotechnol.* **2012**, *7*, 494.
[18] H. Zeng, J. Dai, W. Yao, D. Xiao, X. Cui, *Nat. Nanotechnol.* **2012**, *7*, 490.
[19] K. F. Mak, K. L. McGill, J. Park, P. L. McEuen, *Science* **2014**, *344*, 1489.
[20] G. Y. Wu, N. Y. Lue, Y. C. Chen, *Phys. Rev. B* **2013**, *88*, 125422.
[21] E. J. Sie, J. W. McIver, Y.-H. Lee, L. Fu, J. Kong, N. Gedik, *Nat. Mater.* **2015**, *14*, 290.
[22] M. K. Lee, N. Y. Lue, C. K. Wen, G. Y. Wu, *Phys. Rev. B* **2012**, *86*, 165411.
[23] A. Rycerz, J. Tworzydlo, C. W. J. Bennakker, *Nat. Phys.* **2007**, *3*, 172.
[24] Y. Shimazaki, M. Yamamoto, I. V. Borzenets, K. Watanabe, T. Taniguchi, S. Tarucha, *Nat. Phys.* **2015**, *11*, 1032.
[25] A. M. Jones, H. Yu, N. J. Ghimire, S. Wu, G. Aivazian, J. S. Ross, B. Zhao, J. Yan, D. G. Mandrus, D. Xiao, W. Yao, X. Xu, *Nat. Nanotechnol.* **2013**, *8*, 634.
[26] J. Kim, X. Hong, C. Jin, S.-F. Shi, C. Y. S. Chang, M.-H. Chiu, L.-J. Li, F. Wang, *Science* **2014**, *346*, 1205.
[27] D. Sun, Y. Rao, G. A. Reider, G. Chen, Y. You, L. Brezin, A. R. Harutyunyan, T. F. Heinz, *Nano Lett.* **2014**, *14*, 5625.
[28] C. R. Zhu, K. Zhang, M. Glazov, B. Urbaszek, T. Amand, Z. W. Ji, B. L. Liu, X. Marie, *Phys. Rev. B* **2014**, *90*, 161302.
[29] M. M. Glazov, E. L. Ivchenko, G. Wang, T. Amand, X. Marie, B. Urbaszek, B. L. Liu, *Phys. Status Solidi B* **2015**, *252*, 2349.
[30] J. Xiao, Z. Ye, Y. Wang, H. Zhu, Y. Wang, X. Zhang, *Proc. SPIE* **2015**, *9552*, 95520G.
[31] Y. Luyi, N. A. Sinitsyn, W. Chen, J. Yuan, J. Zhang, J. Lou, S. A. Crooker, *Nat. Phys.* **2015**, *11*, 830.
[32] L. Yang, W. Chen, K. M. McCreary, B. T. Jonker, J. Lou, S. A. Crooker, *Nano Lett.* **2015**, *15*, 8250.
[33] G. Moody, K. Hao, C. K. Dass, A. Singh, L. Xu, K. Tran, C.-H. Chen, M.-Y. Li, L.-J. Li, G. Clark, G. Berghauser, E. Malic, A. Knorr, X. Xu, X. Li, *Proc. SPIE* **2016**, *9746*, 97461T.
[34] M. Selig, G. Berghauser, A. Raja, P. Nagler, C. Schuller, T. F. Heinz, T. Korn, A. Chernikov, E. Malic, A. Knorr, *Nat. Commun.* **2016**, *7*, 13279.
[35] A. Singh, K. Tran, M. Kolarczik, J. Seifert, Y. Wang, K. Hao, D. Pleskot, N. M. Gabor, S. Helmrich, N. Owschimikow, U. Woggon, X. Li, *Phys. Rev. Lett.* **2016**, *117*, 257402.
[36] T. Smolenski, M. Goryca, M. Koperski, C. Faugeras, T. Kazimierczuk, A. Bogucki, K. Nogajewski, P. Kossacki, M. Potemski, *Phys. Rev. X* **2016**, *6*, 021024.
[37] G. Wang, X. Marie, B. L. Liu, T. Amand, C. Robert, F. Cadiz, P. Renucci, B. Urbaszek, *Phys. Rev. Lett.* **2016**, *117*, 187401.
[38] Y. Ye, J. Xiao, H. Wang, Z. Ye, H. Zhu, M. Zhao, Y. Wang, J. Zhao, X. Yin, X. Zhang, *Nat. Nanotechnol.* **2016**, *11*, 598.
[39] P. Dey, L. Yang, C. Robert, G. Wang, B. Urbaszek, X. Marie, S. A. Crooker, *Phys. Rev. Lett.* **2017**, *119*, 137401.
[40] D. H. Kim, D. Lim, *Curr. Appl. Phys.* **2017**, *17*, 321.
[41] E. J. McCormick, M. J. Newburge, Y. K. Luo, K. M. McCreary, S. Singh, I. B. Martin, E. J. Cichewicz Jr., B. T. Jonker, R. K. Kawakami, *2D Mater.* **2017**, *5*, 011010.
[42] T. Yan, S. Yang, D. Li, X. Cui, *Phys. Rev. B* **2017**, *95*, 241406.
[43] Z. Ye, D. Sun, T. F. Heinz, *Nat. Phys.* **2017**, *13*, 26.
[44] C. Zhao, T. Norden, P. Zhang, P. Zhao, Y. Cheng, F. Sun, J. P. Parry, P. Taheri, J. Wang, Y. Yang, T. Scrace, K. Kang, S. Yang, G.-x. Miao, R. Sabirianov, G. Kioseoglou, W. Huang, A. Petrou, H. Zeng, *Nat. Nanotechnol.* **2017**, *12*, 757.
[45] D. Zhong, K. L. Seyler, X. Linpeng, R. Cheng, N. Sivadas, B. Huang, E. Schmidgall, T. Taniguchi, K. Watanabe, M. A. McGuire, W. Yao, D. Xiao, K.-M. C. Fu, X. Xu, *Sci. Adv.* **2017**, *3*, e1603113.
[46] A. Avsar, D. Unuchek, J. Liu, O. L. Sanchez, K. Watanabe, T. Taniguchi, B. Ozyilmaz, A. Kis, *ACS Nano* **2017**, *11*, 11678.
[47] Y. K. Luo, J. Xu, T. Zhu, G. Wu, E. J. McCormick, W. Zhan, M. R. Neupane, R. K. Kawakami, *Nano Lett.* **2017**, *17*, 3877.
[48] J. Lee, S. Bearden, E. Wasner, I. Zutic, *Appl. Phys. Lett.* **2014**, *105*, 042411.
[49] X. Cui, G.-H. Lee, Y. D. Kim, G. Arefe, P. Y. Huang, C.-H. Lee, D. A. Chenet, X. Zhang, L. Wang, F. Ye, F. Pizzocchero, B. S. Jessen, K. Watanabe, T. Taniguchi, D. A. Muller, T. Low, P. Kim, J. Hone, *Nat. Nanotechnol.* **2015**, *10*, 534.
[50] X. Cui, E.-M. Shih, L. A. Jauregui, S. H. Chae, Y. D. Kim, B. Li, D. Seo, K. Pistunova, J. Yin, J.-H. Park, H.-J. Choi, Y. H. Lee, K. Watanabe, T. Taniguchi, P. Kim, C. R. Dean, J. C. Hone, *Nano Lett.* **2017**, *17*, 4781.
[51] L. Wang, I. Meric, P. Y. Huang, Q. Gao, Y. Gao, H. Tran, T. Taniguchi, K. Watanabe, L. M. Campos, D. A. Muller, J. Guo, P. Kim, J. Hone, K. L. Shepard, C. R. Dean, *Science* **2013**, *342*, 614.
[52] K. F. Mak, *Valleytronic Materials, Architectures, and Devices Workshop*, Cambridge, MA, USA **2017**.
[53] J. Kim, C. Jin, B. Chen, H. Cai, T. Zhao, P. Lee, S. Kahn, K. Watanabe, T. Taniguchi, S. Tongay, M. F. Crommie, F. Wang, *Sci. Adv.* **2017**, *3*, e1700518.
[54] A. Mishchenko, J. S. Tu, Y. Cao, R. V. Gorbachev, J. R. Wallbank, M. T. Greenaway, V. E. Morozov, S. V. Morozov, M. J. Zhu, S. L. Wong, F. Withers, C. R. Woods, Y.-J. Kim, K. Watanabe, T. Taniguchi, E. E. Vdovin, O. Makarovsky, T. M. Fromhold, V. I. Fal'ko, A. K. Geim, L. Eaves, K. S. Novoselov, *Nat. Nanotechnol.* **2014**, *9*, 808.